Journal of Physics: Conference Series **3224** (2026) 032089 doi:10.1088/1742-6596/3224/3/032089

Reconsideration of wind farm design and operation based on the two-scale momentum theory

Amanda S M Smyth and Takafumi Nishino
Department of Engineering Science, University of Oxford, Oxford, UK
E-mail: amanda.smyth@eng.ox.ac.uk

Abstract. The importance of atmospheric boundary layer (ABL) interaction with offshore wind farms has become increasingly apparent through many recent studies. ABL interaction effects introduce uncertainty in farm performance predictions, and there is presently a need for robust physics-based models that can be used in preliminary design to quickly evaluate farm performance. This paper employs a recently developed fully analytical model of offshore wind farm aerodynamics based on two-scale momentum theory, which accounts for ABL interaction, wake interaction and realistic rotor performance. The impact of ABL interaction on farm power curves is demonstrated, and the turbine spacing required to achieve a certain target capacity factor (CF) is explored for realistic probability distributions of ABL heights, approximated using the Weibull function. Novel 'ABL-height-informed' control strategies based on optimising the 'farm-scale induction' (the reduction in farm-average wind speed) are also investigated in terms of their impact on the farm power. The achievable farm CF for a given turbine spacing is found to decrease when the expected range of ABL height is lower. The farm power could be somewhat increased by using the new control schemes, which could also significantly reduce the farm-scale induction. This suggests that the farm wake could be reduced while retaining similar or higher farm power.

1. Introduction

The size and number of offshore wind farms is rapidly increasing worldwide. As the number of farms increases and the number of economically viable deployment sites decreases, space-optimised farm design becomes increasingly important. Furthermore, many recent numerical studies have demonstrated the importance of the atmospheric boundary layer (ABL) height on the performance of large wind farms (e.g. [1, 2]): if the ABL height is low it will reduce the power output of the farm, representing a farm-scale power loss due to farm-ABL interaction. While recent numerical studies on ABL interaction effects are mostly for conventionally neutral boundary layers (CNBLs) with a shallow inversion layer of varying strength (e.g. [1, 3]), which may amplify ABL interaction due to gravity waves, the interaction occurs more generally due to change in turbulent mixing of air above the wind farm (and thus the vertical entrainment of momentum and energy into the farm) [4]. Recent studies also suggest that farm-ABL interaction is more closely related to the reduction of 'farm-average' wind speed (i.e. farm-scale induction) rather than to the reduction of 'farm-upstream' wind speed (often referred to as farm-scale blockage or global blockage), and importantly, that the loss due to farm-scale induction can be larger than individual turbine wake losses for large offshore wind farms [3]. As such, a central question for future deployment of large offshore wind farms is how to account for ABL interaction

effects at an early design stage.

A key parameter in the preliminary design stage of large wind farms is turbine spacing or array density, i.e. how many turbines should be installed in a given farm area. For example, Meyers and Meneveau [5] employed the 'top-down' wind farm model of Calaf et al. [6] to predict optimal turbine spacing analytically. They showed that, for a realistic range of 'cost ratios' (i.e. ratio of turbine costs to land costs) the optimal turbine spacing could be considerably larger ($\sim 15D$) than typical spacing ($\sim 7D$); however, their model was for 'infinite' wind farms and did not account for the effects of the farm size or the ABL height explicitly. Nishino and Dunstan [7] proposed a modelling framework called 'two-scale momentum theory', applicable to finite wind farms, which Kirby et al. [8] extended by deriving an analytical model of 'momentum availability factor' to predict how the power of a finite wind farm changes with the farm size and ABL height. This model has been compared successfully with large-eddy simulations (LES) of finite wind farms in CNBLs with different heights [3]. More recently, Nishino and Smyth [9] extended the theory to account for realistic turbine design and farm layout effects explicitly as part of the analytical model.

In this study we demonstrate how the latest version of the analytical two-scale momentum model, outlined recently by Nishino and Smyth [9], can be used to determine the turbine spacing required to achieve a target farm capacity factor (CF). Furthermore, we explore how alternative turbine operational control, based on optimising the farm-average wind speed reduction, can impact overall farm power output and decrease turbine operational loads.

2. Theory

The two-scale momentum theory used in this work is based on applying momentum balance on a control volume containing the whole wind farm [7, 9]. The momentum balance is performed with and without the farm present (variables concerning the latter have the suffix '0'). This analysis framework enables the connection of 'internal' flow modelling (accounting for the characteristics and layout of individual turbines) to 'external' flow modelling (for the interaction of the whole farm and the atmosphere) through a single parameter β, defined as the ratio of the farm-average wind speed (U_F) relative to the wind speed that would occur without the farm present (U_{F0}):

$$\beta \equiv \frac{U_F}{U_{F0}}. \tag{1}$$

The resulting non-dimensional farm momentum (NDFM) equation is:

$$C_T^* \frac{\lambda}{C_{f0}} \beta^2 + \beta^\gamma = M \approx \frac{1 + \frac{h_0}{LC_{f0}}(1 - \beta^2)}{\beta}, \tag{2}$$

where the momentum availability factor M, representing the linear momentum (in the hub-height wind direction) supplied by the atmosphere to the control volume normalised by that of the undisturbed case, is approximated by an analytical model proposed by Kirby et al. [8]. The variable γ is a surface friction exponent, which is set to $\gamma = 2.0$ for the present study, following [7]. The remaining key non-dimensional parameters are the internal thrust coefficient $C_T^* \equiv \Sigma_{i=1}^N T_i / \frac{1}{2}\rho U_F^2 NA$, the effective array density $\lambda/C_{f0} = NA/S_F C_{f0}$, and the effective ABL height h_0/LC_{f0}. These parameters depend on the number of turbines N, the individual turbine thrust T_i and swept area A, the farm surface area S_F, the farm length in the flow direction L, the undisturbed ABL height h_0, and the undisturbed surface friction coefficient C_{f0}. The hub-height air density ρ is assumed constant at 1.204 kg/m^3 in this study.

In order to analyse the farm performance it is necessary to model the relationship between C_T^* and the 'effective' thrust coefficient of all individual turbines in the farm, given by $C_T \equiv \Sigma_{i=1}^N T_i / \frac{1}{2}\rho (U_{T,in})_i^2 NA$, where $U_{T,in}$ is the incoming wind speed upstream of each turbine.

The difference between U_F and $U_{T,in}$ is a function of turbine layout effects, primarily wake effects, and can be quantified through a 'turbine layout factor' χ which we define analytically [9]:

$$\chi \equiv \frac{U_{T,in}}{U_F} = 1 - C_\chi \left[\frac{1 - \sqrt{1 - C_T}}{(1 + 2k\sqrt{\pi/4\lambda})^2} \right] \tag{3}$$

where $k = 0.05$ is a parameter analogous to the wake growth rate in traditional wake models. The empirical parameter C_χ is set to 0.14 for the present study, based on data from an actuator disc (AD) LES study of 50 wind farms with different turbine layouts and wind directions [9]. Then, assuming $C_T^* \approx \chi^2 C_T$ (which is exact if the turbine array is homogeneous), the farm wind-speed reduction factor β can be obtained from equation 2 for a given set of λ/C_{f0}, h_0/LC_{f0} and C_T. In this study we consider the farm density λ as the primary design parameter, and C_T as the turbine control parameter.

In order to represent realistic turbine performance in the analytical framework, as opposed to ideal actuator discs, it is necessary to use a simplified model for rotor aerodynamic performance. Following [9], we estimate C_P as follows:

$$C_P = \left[\frac{\sigma C_P^{\mathrm{Rat}} + (1 - \sigma) C_{P,\mathrm{ADT}}^{\mathrm{Rat}}}{C_{P,\mathrm{ADT}}^{\mathrm{Rat}}} \right] C_{P,\mathrm{ADT}}, \tag{4}$$

where

$$C_{P,\mathrm{ADT}} = \frac{1}{2} C_T \left(1 + \sqrt{1 - C_T} \right), \quad C_{P,\mathrm{ADT}}^{\mathrm{Rat}} = \frac{1}{2} C_T^{\mathrm{Rat}} \left(1 + \sqrt{1 - C_T^{\mathrm{Rat}}} \right), \quad \sigma = \left(\frac{\frac{C_T}{C_{P,\mathrm{ADT}}} - 1}{\frac{C_T^{\mathrm{Rat}}}{C_{P,\mathrm{ADT}}^{\mathrm{Rat}}} - 1} \right)^{\frac{1}{2}}. \tag{5}$$

This approximation takes the turbine rated power and thrust coefficients (C_P^{Rat} and C_T^{Rat}) as inputs, and evaluates C_P for a given operational C_T or vice versa. Evaluation in [9] showed that the model agrees well with aerodynamically optimal rotor performance curves for the DTU 10 MW, IEA 10 MW and IEA 15 MW reference turbines, for the whole range of C_T up to the rated C_T.

Finally, the global farm power coefficient C_{PG} can be obtained from:

$$C_{PG} \equiv \Sigma_{i=1}^{N} \frac{P_i}{\frac{1}{2}\rho U_{F0}^3 NA} = \eta_{ext}\eta_{int}\eta_{rot} C_{P,ADT}, \tag{6}$$

where $C_{P,ADT}$ is the power coefficient obtained by the classical actuator disc theory for a given C_T. The other three variables that determine C_{PG} are the 'external' farm efficiency η_{ext}, the 'internal' farm efficiency η_{int}, and the rotor efficiency η_{rot}. This division of the overall farm efficiency into three coefficients allows for the comparison of the relative importance of 'external' losses due to ABL interaction (through η_{ext}), 'internal' losses caused by turbine-wake interactions (through η_{int}) and losses due to performance of individual rotors (through η_{rot}). It is shown in [9] that $\eta_{ext} = \beta^3$ and $\eta_{int} \approx \chi^3$. The rotor efficiency is defined as $\eta_{rot} = C_P/C_{P,ADT}$, where C_P is the 'effective' power coefficient of all individual turbines in the farm, $C_P \equiv \Sigma_{i=1}^{N} P_i / \frac{1}{2}\rho (U_{T,in})_i^3 NA$. By assuming a large homogeneous farm, such that the effective power coefficient is approximately the same as that of individual turbines in the farm, we can use Equation 4 to find C_P for realistic turbines.

3. Results and discussion

3.1. ABL-height effects on farm performance

Figure 1a shows the predicted global farm power coefficient C_{PG} relative to the rated power coefficient of an individual turbine C_P^{Rat} (0.489 for the IEA 15 MW reference turbine considered

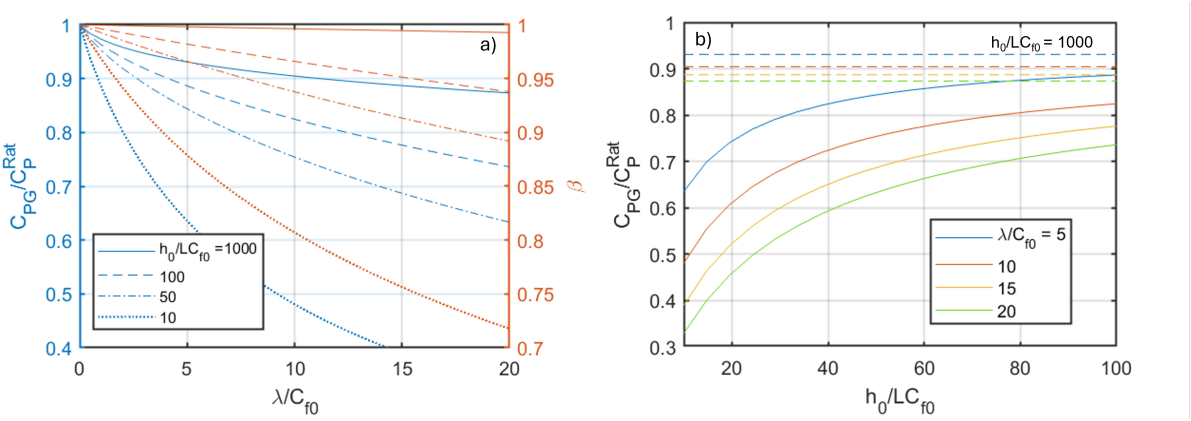

Figure 1. a) Global farm efficiency relative to the rated power coefficient of individual turbines C_P^{Rat} and farm wind-speed reduction factor β as a function of effective array density for different effective ABL heights. b) Global farm efficiency relative to C_P^{Rat} as a function of effective ABL height for different effective array densities.

in this study), as a function of effective array density. The farm wind-speed reduction factor β is also shown, and the results are given for four different effective ABL heights. Throughout this paper the effective ABL height and other normalised quantities are obtained by setting the surface friction coefficient to $C_{f0} = 0.002$ and the farm length to $L = 20$ km. Note that all results in figure 1 are for farms where all turbines are operating aerodynamically optimally at their rated thrust coefficient (that is, $U_{T,in}$ is lower than the rated wind speed U_{Rat} everywhere). In general, it can be seen that both C_{PG} and β decrease with increasing array density, and that this trend becomes stronger at lower ABL heights.

The case with $h_0/LC_{f0} = 1000$ in figure 1a represents a hypothetical scenario where the ABL height is extremely high and thus the atmosphere can supply as much momentum as required to sustain the farm-average wind speed. As a result, $\beta \approx 1$ for all array densities in this case, and the reduction in C_{PG} with increasing array density is relatively small and entirely a function of the layout factor χ, which is dependent on the empirically tuned parameter C_χ. Note that a fixed value of $C_\chi = 0.14$ is used for all cases shown here, representing an average level of wake interaction effects for a regular array of turbines with all wind directions [9]. As the ABL height decreases, C_{PG} decreases substantially due to the reduction in farm-average wind speed seen through the reduction in β, which reduces η_{ext}. This is illustrated further in figure 1b, showing C_{PG} against effective ABL height for different array densities. The horizontal dashed lines represent the asymptotic results at $h_0/LC_{f0} = 1000$ for each array density. Overall, Figure 1 shows that decreasing the effective ABL height has a detrimental effect on farm power.

Figure 2a shows the farm power curves (i.e. power versus the undisturbed wind speed U_{F0}) predicted for different effective array densities and ABL heights. It can be seen that the value of U_{F0} at which the farm reaches the rated power is higher than that for an isolated turbine (black line in figure 2a). This is expected from the reduction of both η_{int} and η_{ext}, but the effect of η_{ext} is substantially stronger. The cases with effective ABL height of 1000 (blue solid and dashed lines, $\beta \approx 1$ and thus $\eta_{ext} \approx 1$) are only slightly shifted from the single turbine power curve. However, for the more realistic ABL heights (red lines) there is a substantial shift in the power curve, and the power output is more sensitive to changes in the array density (compare blue and red dash-dot lines).

This shift in the power curve will negatively impact the farm capacity factor CF, which can be predicted by integrating the product of the farm power curve and the probability density function of U_{F0} at a given site. Here we use a Weibull function with scale and shape parameters

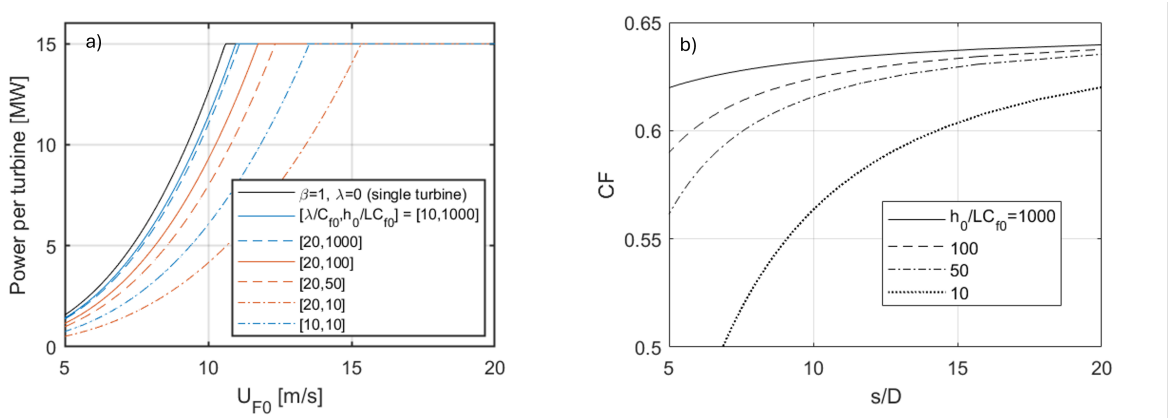

Figure 2. a) Farm power curves for varying effective array densities and ABL heights. b) Non-dimensional turbine spacing s/D $(= \sqrt{\pi/4\lambda})$ required to achieve a given capacity factor CF at a typical offshore wind farm site (with a Weibull distribution of U_{F0} with scale and shape parameters of 11.563 m/s and 2.302) for various effective ABL heights.

of 11.563 m/s and 2.302 (taken from a typical offshore site) as an example. Figure 2b shows the CF as a function of average turbine spacing s/D for different effective ABL heights. The hypothetical case where $\eta_{ext} \approx 1$ is sustained ($h_0/LC_{f0} = 1000$, solid line) has a CF in the range of 0.62 to 0.64 for all turbine spacings considered, the variation being caused by changes in χ due to turbine-wake interaction. However, when the ABL height is more realistic, the CF is more sensitive to the choice of turbine spacing. This suggests that, in an early stage of wind farm design, a typical ABL height seen at the farm site can be used as an input parameter together with the Weibull parameters for U_{F0} to predict the relationship between the CF and turbine spacing (or the number of turbines installed in a given farm area). This relationship is crucial for initial wind farm design as it tells us how the (long-term average) power-per-turbine increases with the turbine spacing, which in turn can be used for preliminary cost-benefit analysis. For example, if a CF of 0.6 is required to reach an economically viable average power-per-turbine, from figure 2b a suitable turbine spacing would be about 7.5 turbine diameters if the typical ABL height is $h_0/LC_{f0} = 50$ (dash-dot line in figure 2b), but about 14 turbine diameters if it is $h_0/LC_{f0} = 10$ (dotted line in figure 2b). This would make a significant difference to the number of turbines in the farm area, and thus the overall power produced.

For realistic farm performance prediction it is more likely that a probability distribution of ABL heights is required to capture the ABL height variation during long periods of time at the target site. While such data is at present limited, qualitative assessment of published data by [10] suggest that Weibull probability distributions could also be representative for the probability of ABL heights. Figure 3a shows three probability distributions for ABL height h_0, estimated from data published by [10] to be representative of realistic offshore sites. The shape parameter is fixed at 3.44, and three different scale parameters λ_s are used as examples of low, medium and high mean ABL height distributions. These distributions can be used to find the resulting farm CF through the following relationship:

$$\mathrm{CF} = \frac{\int\int P(h_0, U_{F0}) p(h_0) q(U_{F0}) dh_0 dU_{F0}}{P^{Rat}}. \tag{7}$$

Here P^{Rat} is the rated turbine power, $P(h_0, U_{F0})$ is the farm power curve as a function of ABL height and undisturbed wind speed (see e.g. Figure 2a) and $p(h_0)$ and $q(U_{F0})$ are the Weibull probability distributions for ABL height and wind speed, respectively. The probability distributions of wind speed and ABL height are assumed to be independent in Equation 7; this

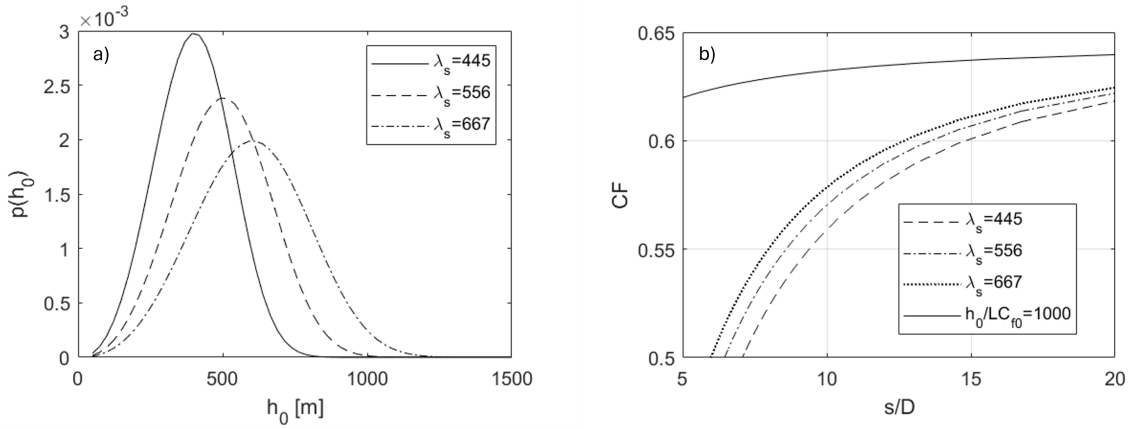

Figure 3. a) Example Weibull probability distributions for the ABL height h_0 (with a fixed Weibull shape parameter of 3.44). b) Non-dimensional turbine spacing s/D ($= \sqrt{\pi/4\lambda}$) required to achieve a given capacity factor CF for different probability distributions of h_0. The probability distribution of U_{F0} is the same as in figure 2b and uncorrelated with the distribution of h_0.

is unlikely to be the case in real life, however there is at present not enough data to model the interdependence of h_0 and U_{F0} at a typical offshore wind farm site. Note that changing wind direction has not been considered for calculations of CF in this paper since we do not consider the effect of wind direction on the turbine layout factor (Equation 3). Figure 3b shows the CF as a function of turbine spacing, using Equation 7 with the Weibull distributions for ABL height shown in Figure 3a, in comparison to that of the hypothetical case with a constant extremely large ABL height (that is $\eta_{ext} \approx 1$, same as in Figure 2b). The Weibull distribution for U_{F0} is the same as that used to obtain the result in Figure 2b. It can be seen that the CF that can be achieved for a certain turbine spacing is substantially lower for the cases that account for ABL height effects, compared to the hypothetical case which neglects the reduction of farm-average wind speed (solid line). There are smaller differences between the individual cases that account for ABL height variation, however there is still a difference of about $s/D = 1$ in turbine spacing between each case to achieve the same CF, and for tightly spaced turbines ($s/D < 10$) the difference in CF for the same turbine spacing is about 0.025-0.04 (that is 5-8% difference in CF). The results in Figure 3 illustrate the importance of including ABL height variation effects in preliminary design stages of large wind farms.

3.2. ABL-height-informed farm control

The results in Figures 1-3 all assume the turbines to be operating using a conventional control scheme: operation at rated power and thrust coefficients until the incoming velocity seen by each turbine $U_{T,in}$ is equal to the rated wind speed (10.6 m/s in this case), above which the turbine operates at the power and thrust coefficients that result in the rated power (15 MW in this case). However, two-scale momentum theory suggests alternative turbine control schemes may improve overall farm performance. Because the global farm power coefficient C_{PG} (Equation 6) is nonlinearly dependent on the farm wind-speed reduction factor β, there is an optimum value β_{opt} at which C_{PG} is maximised for a given ABL height and array density. This is analogous to how the power coefficient of an individual turbine is maximised by operating at the optimal turbine induction factor (resulting in the Betz limit for actuator discs). Equation 2 shows that β is affected by the internal thrust coefficient C_T^*, and thus by the operational thrust coefficient of the individual turbines (since $C_T^* \approx \chi^2 C_T$). As such, it is possible to increase the farm power by operating the turbines at the thrust coefficient that results in β_{opt}, and this optimal thrust coefficient is lower than the rated thrust coefficient.

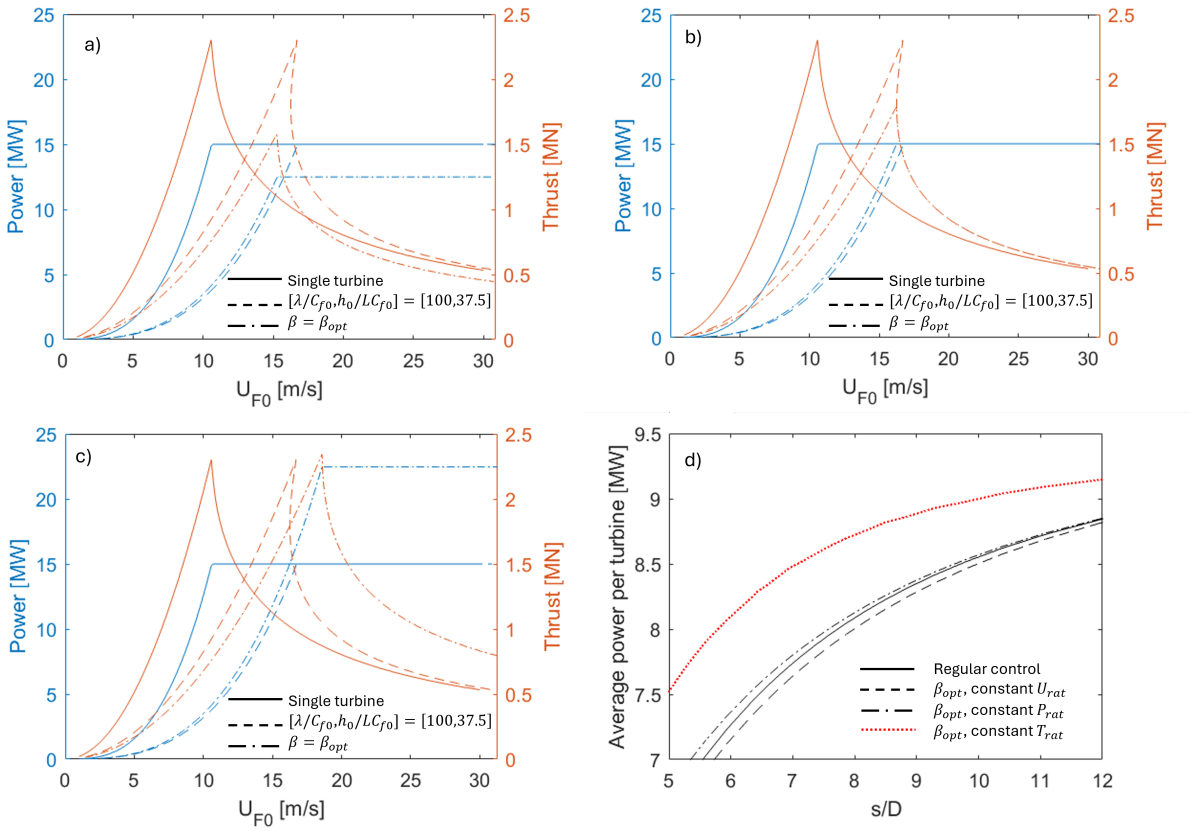

Figure 4. Power curves illustrating alternative control schemes targeting β_{opt}, based on retaining a) rated speed, b) rated power, c) rated peak thrust. Conventional control and performance curves for an isolated turbine (solid line) are included for comparison. d) Average turbine power achieved for the different control schemes, evaluated using the middle probability distribution for h_0 from Figure 3a ($\lambda_s = 556$ m).

To investigate the benefit of targeting β_{opt}, Figure 4a-c illustrates power curves for three different alternative control schemes, showing the power and thrust of a turbine in the farm plotted against the wind speed that would occur without the farm present, U_{F0}. The curves for a turbine in isolation are shown for comparison (solid lines), as well as the curves for conventional control (dashed lines). In Figure 4a-c the array density and ABL heights are kept constant at $\lambda/C_{f0} = 100$ and $h_0/LC_{f0} = 37.5$, in order to more clearly illustrate the impact of the different control options. We consider three novel control options targeting β_{opt}: (I) keep rated speed the same, (II) keep rated power the same, (III) keep rated thrust the same. It is not possible to combine these without changing the turbine design. Note that, as will be shown below, option (III) would require a larger generator size than the original 15 MW, whereas options (I) and (II) are achievable without changing the generator size.

Figure 4a shows option (I): below rated speed (that is, when $U_{T,in} < 10.6$ m/s) the turbine is operated at the C_T which results in β_{opt}. This C_T is lower than the rated C_T. At and above rated speed, the power is kept constant by reducing C_T accordingly. It can be seen that the alternative control scheme (dash-dot lines) does result in an increased power output in below-rated conditions, relative to conventional control. However, since a lower C_T also implies a lower C_P, the turbine does not reach the original rated power of 15 MW at the rated speed, and instead produces around 13 MW at and above it. The thrust on the turbine can also be seen to be substantially lower for the alternative control scheme, compared to standard control.

Furthermore, this control scheme reaches rated speed at lower U_{F0} compared to standard control, implying that the farm induction is successfully reduced in the new scheme.

Figure 4b shows option (II): the turbine operates at C_T resulting in β_{opt} until reaching the rated power of 15 MW. This requires an increase in the rated speed, due to the reduction in C_P that corresponds with operation at lower-than-rated C_T. Note that the rated speed required to achieve a rated power of 15 MW depends on the array density and ABL height if β_{opt} is targeted, and the required rated speed would thus change between different farms and environmental conditions (see Figure 5b below). The alternative control scheme can again be seen to produce more power than standard control for the same U_{F0}, and reaches rated power at lower U_{F0} compared to standard control. Again, the peak turbine thrust of the alternative control scheme is lower than for standard control.

Figure 4c shows option (III): the turbine keeps operating at C_T corresponding to β_{opt} until reaching the same peak thrust as the original control scheme, after which the power is kept constant. This results in a new rated power of about 22.5 MW. This large increase in rated power would not be feasible while retaining the same generator as that used for a turbine rated at 15 MW, and this control scheme would thus require a turbine redesign. However, it illustrates the potential scope for increased power through alternative control with regards to rated turbine thrust as the limiting load condition.

Note that all the alternative control options in Figure 4a-c result in a lower farm induction than what would be achieved with regular control. This means that the farm-average wind speed is higher for the alternative control cases than for the conventional control. As β is closely connected to the strength of the farm wake, the alternative control schemes can also potentially reduce the downstream impact of the wind farm while retaining the same or higher power output.

Figure 4d shows the average power per turbine achieved for different turbine spacings when using standard and the three alternative control schemes, using the middle Weibull distribution in Figure 3a ($\lambda_s = 556$ m) for the ABL height probability. The probability distribution of U_{F0} is the same as that used earlier in Figure 2b. It can be seen that option (I) of optimising β while keeping the rated speed the same (dashed line) produces slightly less power than standard control (solid line), due to the reduction in power produced above rated speed: at a turbine spacing of $8D$, for example, option (I) produces 1% less power than the conventional control. However, option (II) of keeping rated power the same while operating at β_{opt} (dash-dot line) gives slightly more power than standard control, especially when turbines are closely spaced: at $8D$ turbine spacing option (II) produces almost identical power to conventional control, but at $5.6D$ spacing it produces about 1.5% more power. This improvement is due to the increased power produced in below-rated conditions, and the fact that rated power is reached at lower U_{F0}. Option (III) of keeping rated peak turbine thrust the same (red dotted line) produces substantially higher power on average than the other schemes, due to the higher rated power that is reached: at $8D$ turbine spacing option (III) produces about 7.5% more power than conventional control. Note that while the differences in power produced by control options (I) and (II) are modest, this power is produced at a substantially lower turbine thrust, which may have benefits to turbine longevity as well as for reduction of the farm wake.

The effects of ABL interaction and the impact of alternative control can be further illustrated by the farm-upstream wind speed U_{F0} at which the farm reaches rated power, that is the 'rated' U_{F0}. This occurs at velocities higher than the rated velocity of individual turbines, due to both wake effects and ABL interaction effects. Figure 5a shows how the rated U_{F0} varies with the effective ABL height for different array densities, using both regular control (solid lines) and control to target β_{opt} while retaining the rated power at 15 MW (control option (II), dashed lines). As expected, the rated U_{F0} increases with increasing array density and decreasing ABL height. It can be seen that alternative control targeting β_{opt} consistently lowers the rated U_{F0}, especially at lower ABL heights. This lowering of the rated U_{F0} in the alternative control case is

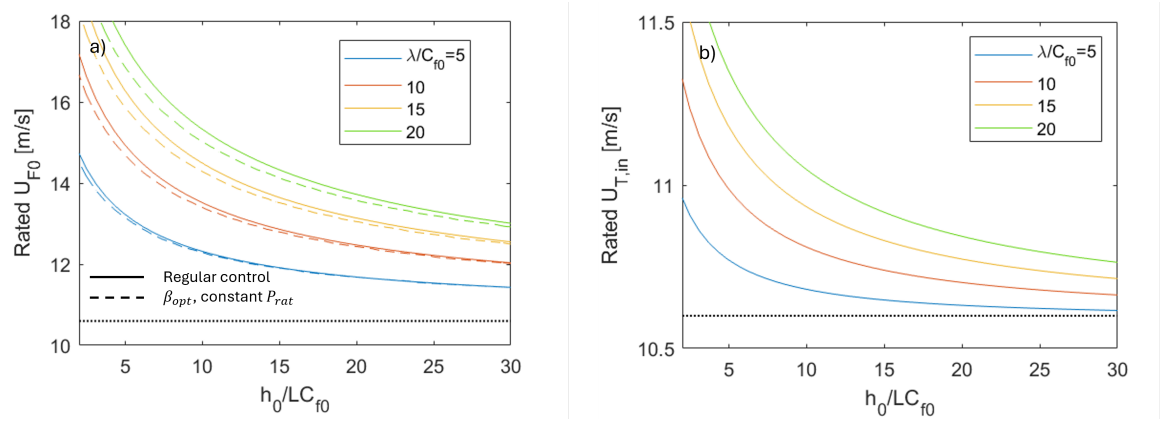

Figure 5. a) Undisturbed (farm-upstream) wind speed required for the farm to reach rated power, for regular control and when using the control scheme illustrated in Figure 4b (control scheme (II)). b) Inflow (turbine-upstream) speed required for a turbine in the farm to achieve a rated power of 15 MW when using control scheme (II). The dotted horizontal line indicates the original rated speed of 10.6 m/s.

relatively small, however the difference between the regular and novel control cases is diminished by the fact that the rated inflow speed to the turbine $U_{T,in}$ which is required to reach 15 MW for control option (II) also increases with increasing array density and decreasing ABL height. Figure 5b shows the variation in rated $U_{T,in}$ that is required to reach 15 MW with control option (II) with changing ABL height for different array densities. The new rated $U_{T,in}$ can be seen to be higher than the regular rated speed of 10.6 m/s especially for low ABL heights and high farm densities. This increase in rated $U_{T,in}$ also results in increased rated U_{F0} in Figure 5a for the alternative control case, making the difference in rated U_{F0} between the alternative and regular control schemes more subtle.

3.3. Discussion

The set of analytical models used in this paper, described in more detail in [9], allows for quick preliminary analysis of potential sites for wind farm development, accounting for both turbine-wake and farm-ABL interaction effects on performance outcomes. The underlying theoretical framework is versatile and comprehensive, relying on standard control volume momentum balance applied to the entire farm. It can thus be applied to realistic finite-size offshore wind farms. However, certain assumptions have been used in order to derive the specific closed-form analytical sub-models used in this paper and in [9], which should be noted when interpreting the results.

This paper uses the notation C_T to represent the effective thrust coefficient of all individual turbines in the farm, defined as $C_T \equiv \Sigma_{i=1}^{N} T_i / \frac{1}{2}\rho(U_{T,in})_i^2 NA$. Thus, the control of C_T in Section 3.2 used to achieve β_{opt} can be seen as farm-average C_T-control. For large homogeneous farms with uniform inflow, the thrust coefficients of individual turbines are approximately the same, in which case this C_T is approximately the same as the thrust coefficient of individual turbines in the farm.

The basic framework of two-scale momentum theory is applicable to any offshore wind farms, however certain assumptions in the present set of analytical models (such as the approximations $C_T^* \approx \chi^2 C_T$ and $\eta_{int} \approx \chi^3$) are only applicable to large (but finite-sized) homogeneous wind farms. A farm is here considered 'large' when its length is at least an order of magnitude larger than the ABL height. Furthermore, transient effects due to e.g. rapid changes in farm-average wind speed and direction are not considered in the present model.

The layout factor χ represents the difference between the farm-average wind speed and the wind speed upstream of individual turbines in the farm, which is mostly due to turbine-wake interactions and is a function of the exact turbine layout. There are many ways to obtain this parameter, including numerical simulations and engineering wake models. In order to obtain a closed-form analytical approach while explicitly accounting for the dependence of χ on both C_T and the array density, the form in Equation 3 is adopted here and in [9]. The layout factor is then dependent on the empirical coefficient C_χ. For homogeneous large farms, C_χ is related to the degree of 'overlap' of frontal projected areas of rotors between subsequent turbine rows (which is a function of the wind direction): C_χ approaches 0 for no overlap between subsequent rows and 1 for fully aligned rows. While this interpretation is not exact, it provides a physical basis for the empirical constant. Comparison to numerical simulations in [9] confirmed C_χ to be approximately in the range 0 to 1, and suggested $C_\chi = 0.14$ as a representative average value for typical offshore wind farms. As such, $C_\chi = 0.14$ was used throughout this study. However, this is not necessarily a representative value for all wind farms.

The analytical model for the momentum availability factor M on the right-hand side of Equation 2 takes the ABL height h_0 as the sole atmospheric parameter. This relies on certain assumptions of the behaviour of the ABL, most notably on assuming a linear profile of shear stress. An alternative model for M that does not assume a linear shear stress profile and takes the Rossby number as an additional input parameter was recently developed by Baungaard et al. [11], which expands the applicability of the analytical model also to ABLs with strong veering due to the Coriolis force. The strength of the inversion layer has been demonstrated not to strongly affect the total value of M [3], while the effect of inversion layer thickness on M has not yet been evaluated explicitly. It should also be noted that the validity of the present model of M for scenarios when h_0 is less than the turbine height has not been fully confirmed. While this is not an issue for the majority of cases presented in this paper, the probability distributions of h_0 considered in Figure 3a and related analysis include values of h_0 which could be less than the turbine height. Preliminary analysis using LES data by Kirby et al. [3] suggests the model still performs reasonably well even when h_0 is less than the turbine height, however further study is required to confirm the full validity of the present model for M in such instances.

While only the objective of maximising power through ABL-informed farm control has been considered explicitly in Section 3.2, other control objectives could be considered as well. For example, the farm wind-speed reduction factor β is strongly related to the strength of the farm wake. Since the alternative control schemes presented in Section 3.2 are based on operating turbines at lower-than-rated C_T, the corresponding β will be higher than what would occur in regular control. As a result, the farm wake will likely be reduced while retaining the same or higher farm power output, compared to the regular control case. Furthermore, if environmental regulations or interference with downstream farms will require curtailment of the farm wake, the two-scale theory framework suggests it is possible to control C_T to achieve a target farm β, and thus a target farm wake deficit. This is a possible topic for future studies.

4. Conclusions

This paper has demonstrated the use of two-scale momentum theory with analytical sub-models to quickly evaluate the performance of large wind farms. The analytical model accounts for realistic turbine performance curves, turbine layout effects (related to turbine-wake interaction) and ABL interaction effects. The Weibull function has been adopted to model probability distributions of ABL height and farm-upstream wind speed, in order to investigate their impact on the farm's long-term capacity factor. The results show the importance of ABL interaction effects on farm power and capacity factor. The achievable capacity factor can be significantly lower when the ratio of ABL height to farm length is low, and the turbine spacing required to achieve a certain capacity factor can be significantly larger.

The key impact of ABL interaction in this analytical model is on the 'farm-scale induction' (that is the farm-average wind speed reduction), and it was demonstrated that increased farm power could be achieved through novel 'ABL-height-informed' turbine control schemes that optimise the farm-scale induction for maximum power output. Furthermore, the optimal farm-scale induction could be significantly smaller than the induction achieved when using regular control, suggesting that the farm-average wind speed could be increased (which correlates to reduced strength of the farm wake) while retaining the same or higher farm power. Overall, the analytical model presented in this paper is promising for use in early-stage quick evaluation of farm performance, and for exploring alternative control schemes for maximising the farm power and/or reducing the farm wake.

References

[1] Lanzilao L and Meyers J 2024 A parametric large-eddy simulation study of wind-farm blockage and gravity waves in conventionally neutral boundary layers *J. Fluid Mech.* **979** A54 URL https://doi.org/10.1017/jfm.2023.1088

[2] Ivanell S, Chanprasert W, Lanzilao L, Bleeg J, Meyers J, Mathieu A, Juhl Andersen S, Mouradi R S, Dupont E, Olivares-Espinosa H and Troldborg N 2025 An inter-comparison study on the impact of atmospheric boundary layer height on gigawatt-scale wind plant performance *Wind Energ. Sci. Discuss. [preprint]* URL https://doi.org/10.5194/wes-2025-88

[3] Kirby A, Nishino T, Lanzilao L, Dunstan T D and Meyers J 2025 Turbine- and farm-scale power losses in wind farms: an alternative to wake and farm blockage losses *Wind Energ. Sci.* **10** 435–450 URL https://doi.org/10.5194/wes-10-435-2025

[4] Porté-Agel F, Bastankhah M and Shamsoddin S 2020 Wind-turbine and wind-farm flows: a review *Boundary-Layer Meteorol.* **174** 1–59 URL https://doi.org/10.1007/s10546-019-00473-0

[5] Meyers J and Meneveau C 2012 Optimal turbine spacing in fully developed wind farm boundary layers *Wind Energy* **15** 305–317 URL https://doi.org/10.1002/we.469

[6] Calaf M, Meneveau C and Meyers J 2010 Large eddy simulation study of fully developed wind-turbine array boundary layers *Physics of Fluids* **22** 015110 URL https://doi.org/10.1063/1.3291077

[7] Nishino T and Dunstan T D 2020 Two-scale momentum theory for time-dependent modelling of large wind farms *J. Fluid Mech.* **894** A2 URL https://doi.org/10.1017/jfm.2020.252

[8] Kirby A, Dunstan T D and Nishino T 2023 An analytical model of momentum availability for predicting large wind farm power *J. Fluid Mech.* **976** A24 URL https://doi.org/10.1017/jfm.2023.844

[9] Nishino T and Smyth A S M 2025 Power loss mechanisms and optimal induction factors for realistic large wind farms *[preprint]* URL https://doi.org/10.48550/arXiv.2508.02727

[10] Adams N, Rodaway C, Gottschall J, Hawkes G and Simon E 2023 OWA GloBE: Building industry consensus on the global blockage effect in offshore wind *Presentations from the Wind Energy Science Conference 2023 Mini-Symposium* URL https://doi.org/10.5281/zenodo.8085204

[11] Baungaard M, Nishino T and Kirby A 2026 Validation and extension of an analytic momentum availability model for the two-scale momentum theory of wind farm flows *[preprint]* URL https://doi.org/10.48550/arXiv.2602.10126